Low-Melting, Mononuclear Tetrahydrofuran Complexes of M(2,2,6,6-tetramethylheptane-3,5-dionate)$_2$ (M = Ba, Sr) and Related Analogues

Witold Paw,*,† Thomas H. Baum,† Kin-Chung Lam,‡ and Arnold L. Rheingold‡

ATMI, Inc., 7 Commerce Drive, Danbury, Connecticut 06810, and Department of Chemistry and Biochemistry, University of Delaware, Newark, Delaware 19716

Received June 2, 1999

Introduction

Metal oxide thin films continue to attract significant attention due to their potential for future microelectronics applications.[1] Many oxide materials contain group II elements such as barium and strontium. Examples include superconductors ($YBa_2Cu_3O_7$), high dielectric constant oxides ($Ba_xSr_{1-x}TiO_3$), and ferroelectric materials ($SrBi_2Ta_2O_9$), the latter two materials being considered for high-density memory capacitors. These thin-film materials may be deposited by chemical vapor deposition (CVD) using appropriate precursors and liquid delivery techniques. The deposition of conformal films is required for large-scale manufacturing of high-density devices. Research efforts have utilized both fluorinated and nonfluorinated group II CVD precursors containing alkoxide, β-diketonate, and related ligands. Fluorinated sources exhibit higher vapor pressures, but deposited films are typically contaminated by fluoride impurities.[2−4] Nonfluorinated precursors, however, display lower volatility, resulting from their multinuclear nature, and present a significant challenge for the reproducible delivery and transport to the CVD reactor.

The chemical synthesis of novel group II sources designed specifically for CVD has led to the detailed examination of various precursors. Both inter- and intramolecular stabilizations of the metal centers were examined.[5−13] The production of liquid precursors was thought to enhance the volatilities of these materials and simplify their delivery. In a different approach, H_2O, THF, NH_3, and NEt_3 were added to the carrier gas stream to enhance the vapor pressures of the Ba(β-diketonate)$_2$ complexes.[14−16] The improved transport observed was rationalized in terms of Lewis base adduct formation and stabilization of low-nuclearity species. For example, $[Ba(thd)_2(NH_3)_2]_2$ was structurally characterized in the solid state and found to exist as a dinuclear species with NH_3 coordination to the $Ba(thd)_2$ core.[17] For comparison, $[Ba(thd)_2]_x$ was shown to be tetranuclear in the solid state.[18,19]

In this report, we present recent structural determinations of THF-adducted $Ba(thd)_2$ and $Sr(thd)_2$ precursors, specifically $Ba(thd)_2(THF)_4$ and $Sr(thd)_2(THF)_4$. These structures are compared to those of complexes containing different Lewis base species. Our studies were motivated by the increased interest in using THF as a solvent for the liquid delivery CVD of BST.[20] Interestingly, the solubilities of $[Ba(thd)_2]_x$ in THP (tetrahydropyran) and THF gave surprisingly different values, suggesting the formation of different species in each of these systems. Moreover, crystalline THP and THF complexes were easily obtained in contrast to the typical powdery appearance of $[Ba(thd)_2]_x$. Solvent adduct formation is not unexpected, since numerous THF adducts of group II metals are known. Furthermore, the syntheses of $[Ba(thd)_2]_x$ and $[Sr(thd)_2]_x$ seem to proceed readily in THF when compared to hydrocarbon solvents indicating direct interactions of solvent molecules with the metal centers.

Experimental Section

Physical Measurements. ^{1}H NMR spectra were recorded on a Varian Gemini 200 MHz spectrometer. Thermal analyses (STA = TGA (thermogravimetric analysis) + DSC (differential scanning calorimetry) were carried out on a Rheometric Scientific STA1000+ apparatus under argon atmosphere with 25 mL/min flow and 10 °C/min heating rate. Elemental analyses (C, H) were performed by Quantitative Technologies, Inc., Whitehouse, NJ. Melting points were determined on a MEL-TEMP apparatus.

Materials and Procedures. Hexane, pentane, diethyl ether, and THF were distilled from sodium benzophenone ketal. THP was obtained from Aldrich and used as received. $[Ba(thd)_2]_x$ was synthesized from Ba and Hthd in anhydrous THF. $[Sr(thd)_2]_x$ was prepared from Sr and Hthd in anhydrous hexanes using methanol as a catalyst.

Syntheses and Characterizations. All complexes were formed by dissolution of $[Ba(thd)_2]_x$ and $[Sr(thd)_2]_x$ in the appropriate solvent. X-ray-quality crystals of $Ba(thd)_2(THF)_4$ and $Sr(thd)_2(THF)_4$ were grown from concentrated solutions upon cooling to −20 °C. $[Ba(thd)_2(THP)_2]_x$ and $[Sr(thd)_2(THP)_2]_x$ precipitated upon cooling concentrated solutions that were heated to 60 °C. $[Ba(thd)_2(Et_2O)]_2$ precipitated spontaneously upon dissolution of $[Ba(thd)_2]_x$ in Et_2O, while $[Sr(thd)_2(Et_2O)]_2$ precipitation required cooling of the concentrated solution. All

† ATMI, Inc.
‡ University of Delaware.

(1) *Encyclopedia of Inorganic Chemistry*; King, R. B., Ed.; Wiley: Chichester, England, 1994.
(2) Mizushima, Y.; Hirabayashi, I. *J. Mater. Res.* **1996**, *11*, 2698.
(3) Shamlian, S. H.; Hitchman, M. L.; Cook, S. L.; Richards, B. C. *J. Mater Chem.* **1994**, *4*, 81.
(4) Gardiner, R. A.; Brown, D. W.; Kirlin, P. S.; Rheingold, A. L. *Chem. Mater.* **1991**, *3*, 1053.
(5) Drake, S. R.; Miller, S. A. S.; Williams, D. J. *Inorg. Chem.* **1993**, *32*, 3227.
(6) Schulz, D. L.; Hinds, B. J.; Neumayer, D. A.; Stern, C. L.; Marks, T. J. *Chem. Mater.* **1993**, *5*, 1605.
(7) Norman, J. A. T.; Pez, G. P. *J. Chem. Soc., Chemm. Commun.* **1991**, 971.
(8) Schwarberg, J. E.; Sievers, R. E.; Moshier, R. W. *Anal. Chem.* **1970**, *42*, 1828.
(9) Iljina, E.; Korjeva, A.; Kuzmina, N.; Trojanov, S.; Dunaeva, K.; Martynenko, L. *Mater. Sci. Eng.* **1993**, *B18*, 234.
(10) Marks, T. J. *Pure Appl. Chem.* **1995**, *67*, 313.
(11) Caulton, K. G.; Chisholm, M. H.; Drake, S. R.; Folting, K.; Huffman, J. C.; Streib, W. S. *Inorg. Chem.* **1993**, *32*, 1970.
(12) Tesh, K. F.; Burkey, D. J.; Hanusa, T. P. *J. Am. Chem. Soc.* **1994**, *116*, 2409.
(13) Gordon, R. G.; Chen, F.; Diceglie, N. J. Jr.; Kenigsberg, A.; Liu, X.; Teff, D. J.; Thornton. Presented at the Materials Research Society Symposium Proceedings, Boston, MA, Dec 1997; paper W7.3.
(14) Matsuno, S.; Urchikawa, F.; Yoshizaki, K. *Jpn. J. Appl. Phys.* **1990**, *29*, L947.
(15) Zhao, J.; Dahmen, K.-H.; Marcy, H. O.; Tonge, L. M.; Marks, T. J.; Wessels, B. W. *Appl. Phys. Lett.* **1988**, *53*, 1750.
(16) Zhao, J.; Marcy, H. O.; Tonge, L. M.; Marks, T. J.; Kannewurf, C. R. *Physica C* **1989**, *159*, 710.
(17) Rees, W. S., Jr.; Carris, M. W.; Hesse, W. *Inorg. Chem.* **1991**, *30*, 4479.
(18) Gleizes, A.; San-Lenain, S.; Medus, D. *C. R. Acad. Sci. Paris, Ser. II* **1991**, *313*, 761.
(19) Drake, S. R.; Hursthouse, M. B.; Abdul Malik, K. M.; Otway, D. J. *I. Chem. Soc., Dalton. Trans.* **1993**, 2883.
(20) Kawahara, T.; Makita, T.; Matsuno, S.; Tsutahara, K.; Doi, N.; Yuki, A.; Sanko, M.; Mikami, N.; Matsui, Y., et. al. Jpn. Kokai Tokkyo Koho, JP 07268634 A2, 1995, Mitsubishi Electric Corp.

10.1021/ic990641z CCC: $19.00
Published on Web 04/04/2000

Table 1. Crystallographic Data for $Ba(thd)_2(THF)_4$ and $Sr(thd)_2(THF)_4$

formula	$C_{38}H_{70}O_8Ba$	$C_{38}H_{70}O_8Sr$
fw	792.28	742.56
space group	*I*2/*a*	*I*2/*a*
a (Å)	19.9003(4)	19.9087(3)
b (Å)	9.5492(2)	9.6863(20)
c (Å)	23.6351(4)	23.0043(5)
α (deg)	90	90
β (deg)	109.3708(10)	109.2415(9)
γ (deg)	90	90
V (Å^3)	4237.15(15)	4188.4(2)
Z	4	4
cryst color, habit	colorless block	colorless plate
D_{calc} (g/cm^3)	1.242	1.178
λ (Å)	0.710 73	0.710 73
T (K)	173(2)	173(2)
μ (mm^{-1})	0.981	1.331
R1, wR2 [$I > 2\sigma(I)$][a]	0.0761, 0.2062	0.0685, 0.1668
R1, wR2 (all data)	0.1001, 0.2291	0.0930, 0.1849

[a] $R1 = \sum||F_o| - |F_c||/\sum|F_o|$. $wR2 = [\sum[w(F_o^2 - F_c^2)^2]/\sum[w(F_o^2)^2]]^{1/2}$.

complexes were characterized by ^{1}H NMR in C_6D_6 and thermal analyses of the solids: $Ba(thd)_2(THF)_4$, 5.91 (s, 2H, −CH), 3.60 (m, 8H, $-CH_2$), 1.43 (m, 8H, $-CH_2$), 1.22 (s, 36H, $-CH_3$); $Sr(thd)_2(THF)_4$, 5.88 (s, 2H, −CH), 3.60 (m, 8H, $-CH_2$), 1.43 (m, 8H, $-CH_2$), 1.26 (s, 36H, $-CH_3$). Elemental analyses for $[Ba(thd)_2(THP)_2]_x$ and $[Sr(thd)_2(THP)_2]_x$ were also obtained. Calcd for $[Ba(thd)_2(THP)_2]_x$: C, 56.84; H, 8.65. Found: C, 56.54; H, 8.71. Calcd for $[Sr(thd)_2(THP)_2]_x$: C, 61.36; H, 9.33. Found: C, 61.41; H, 9.43. Melting point measurements yielded the following values: $Ba(thd)_2(THF)_4$, 25 °C; $Sr(thd)_2(THF)_4$, 30 °C; $[Ba(thd)_2(THP)_2]_x$, 66 °C; $[Sr(thd)_2(THP)_2]_x$, 77 °C. Melting points of $[Ba(thd)_2(Et_2O)]_2$ and $[Sr(thd)_2(Et_2O)]_2$ could not be determined and were crudely estimated from thermal analyses; they ranged from 60 to 100 °C.

Crystallographic Structural Determinations. Crystal, data collection, and refinement parameters for $Ba(thd)_2(THF)_4$ and $Sr(thd)_2(THF)_4$ are given in Table 1. A colorless block of $Ba(thd)_2(THF)_4$ and a colorless plate of $Sr(thd)_2(THF)_4$ were selected and mounted with epoxy cement on thin glass fibers. The data for all structures were collected on a Siemens P4 diffractometer equipped with a SMART/CCD detector and an LT2 cooling system. The systematic absences in the diffraction data are compatible with the space groups *Ia* and *I*2/*a* for both structures. The value of *Z* and the presences of a 2-fold axis supported the centrosymmetric option and yielded chemically reasonable and computational stable refinements. The structures were solved using direct methods, completed by subsequent difference Fourier syntheses, and refined by full-matrix least-squares procedures. The structures are isomorphous. DIFABS1 absorption correction was applied to the data of $Sr(thd)_2(THF)_4$. All non-hydrogen atoms were refined with anisotropic displacement coefficients, and all hydrogen atoms were treated as idealized contributions. All software and sources of the scattering factors are contained in the SHELXTL (5.10) program library (G. Sheldrick, Siemens XRD, Madison, WI).

Results

THF Complexes. Crystalline samples of $Ba(thd)_2(THF)_4$ and $Sr(thd)_2(THF)_4$ displayed unusually low melting points of 25 and 30 °C, respectively. These values explain the relatively high solubilities of $[Ba(thd)_2]_x$ and $[Sr(thd)_2]_x$ in THF at room temperature. The low melting points and high solubilities were both indicative of THF adduct formation. This was confirmed by X-ray cystallographic analysis of the purified solids isolated by cooling concentrated THF solutions, as shown in Figures 1 and 2. Both complexes are mononuclear, containing four THF ligands positioned within the equatorial plane between the thd ligands. Such a geometry is not surprising in light of the previous reports on Lewis base adducts of $Ba(thd)_2$ and $Sr(thd)_2$; in many of these adducts, the Lewis base occupies the equatorial

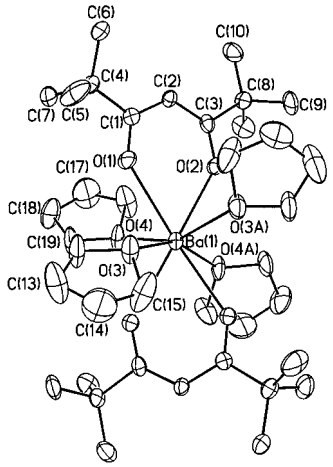

Figure 1. ORTEP diagram of $Ba(thd)_2(THF)_4$.

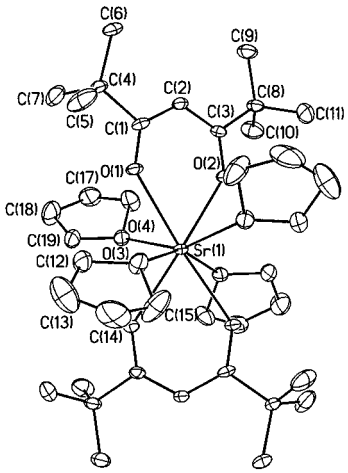

Figure 2. ORTEP diagram of $Sr(thd)_2(THF)_4$.

plane,[21,22] analogous to the THF molecules in $Ba(thd)_2(THF)_4$ and $Sr(thd)_2(THF)_4$. It is surprising, however, that the THF ligands can stabilize a mononuclear structure. The tendency of $Ba(thd)_2$ and $Sr(thd)_2$ to oligomerize is well established, and relatively strong Lewis base donors, such as tetraglyme, are required to stabilize the mononuclear structures.

Simultaneous thermal analysis (STA), a combination of thermal gravimetric analysis (TGA) and differential scanning calorimetry (DSC), was performed on $Sr(thd)_2(THF)_4$ (Figure 3). The THF ligands dissociate easily from the complexes even at relatively low temperatures (<40 °C). The analyses also indicated that at least two THF ligands were present per metal atom and they were readily liberated below 150 °C. In addidion, $[M(thd)_2]_x$ was formed upon loss of THF, as indicated by the presence of characteristic melting endotherms for each chemical species. It was also noticed that THF loss occurs at room temperature under a nitrogen flow.

The NMR resonances of thd and THF ligands were typical, and the chemical shifts for the latter were virtually undistinguishable from those of free THF molecules. Thus no conclusion about the existence of ligand exchange in solution can be drawn from these simplest NMR measurements. However, some evidence of dynamic behavior came from the measurements with varying THF content. The ^{1}H NMR spectra of the $[Sr(thd)_2]_x$/

(21) Drake, S. R.; Miller, S. A. S.; Williams, D. J. *Inorg. Chem.* **1993**, *32*, 3227.
(22) Gardiner, R. A.; Gordon, D. C.; Stauf, G. T.; Vaartstra, B. A.; Ostrander, R. L.; Rheingold, A. L. *Chem. Mater.* **1994**, *6*, 1967.

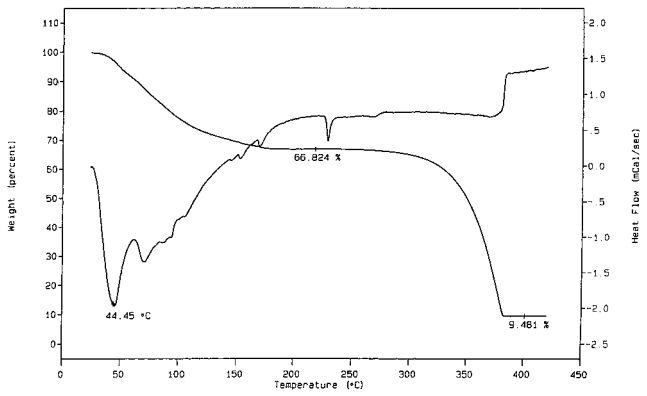

Figure 3. TGA and DSC plots of $Sr(thd)_2(THF)_4$ obtained simultaneously in 1 atm of argon flowed at 25 sccm at a temperature program rate of 10 °C/min.

THF mixtures exhibited broadened thd resonances at intermediate THF content (0.5−3.5 mol of THF/mol of Ba species). Upon addition of excess THF, the thd resonances became sharper and no new THF resonances were noted. No significant changes in chemical shifts (>0.1 ppm) were observed also in this case.

THP Complexes. The thermal analysis of the THP adduct of $Ba(thd)_2$ displayed an initial weight loss of 25.4% at temperatures below 100 °C. This weight loss agrees well with the molecular formula $Ba(thd)_2(THP)_2$, which contains 25.5% of THP. The ^{1}H NMR spectrum displayed a THP to thd resonance ratio that was consistent with this formulation. The melting point of $Ba(thd)_2(THP)_2$ was determined as 66 °C, while the Sr analogue's melting point was 77 °C. Given these physical similarities, the structures of both THP complexes are thought to be identical. It should be noted that these melting points are not sharp, even though highly pure, crystalline samples were used for both measurements. Elemental analyses of both species displayed excellent agreement with values calculated for $M(thd)_2(THP)_2$. Each material displayed dramatically lower solubility in THP at room temperature (0.13 M for the Ba complex) when compared to dissolution in THF (>0.75 M for the Ba complex).

Different ligand-to-metal ratios, melting points, and solubilities in the coordinating solvents are strong evidence for the different molecular structures (nuclearities) adopted by the individual complexes.

Et_2O Complexes. The structure of the diethyl ether adduct of $Ba(thd)_2$ has been previously reported.[23] The molecule's structure is dinuclear with one Et_2O molecule per metal center, $[Ba(thd)_2(Et_2O)]_2$. It is assumed that the Sr analogue displays an identical structure, and the data below support this assumption. The STA plots of the diethyl ether complexes display initial weight loses (below 120 °C) that agree well with the presence of one ether molecule per metal atom in each case. $[Ba(thd)_2(Et_2O)]_2$: STA, 12.5%; theor, 12.8%. $[Sr(thd)_2(Et_2O)]_2$, STA, 11.8%; theor, 14.0%. Melting points of these complexes could not be determined accurately, as partial melting of the Ba complex was noticed around 80 °C, but the material never fully melted. At temperatures well above 50 °C, the liberation of ether is very fast and the byproducts with fewer Et_2O ligands are expected to possess higher melting points. However, the broad endotherms observed during thermal analyses of these complexes suggest that the melting points are between 60 and 100 °C.

(23) Rosetto, G.; Polo, A.; Benetollo, F.; Porchia, M.; Zanella, P. *Polyhedron* **1992**, *11*, 979.

Discussion

The accumulated experimental results indicate that the ether adducts of $Ba(thd)_2$ and $Sr(thd)_2$ depend strongly on the identities of the Lewis base ligands. While the THF complexes are mononuclear, the THP and Et_2O adducts are dinuclear. The previously reported ammonia adduct of $Ba(thd)_2$, $[Ba(thd)_2(NH_3)_2]_2$,[17] exhibits the same ligand-to-metal ratio and is believed to have a similar structure to that of the THP adducts. Similarity of the melting points for the THP and Et_2O adducts also suggests that they possess similar molecular structures. The experimentally determined and proposed structures are depicted as follows:

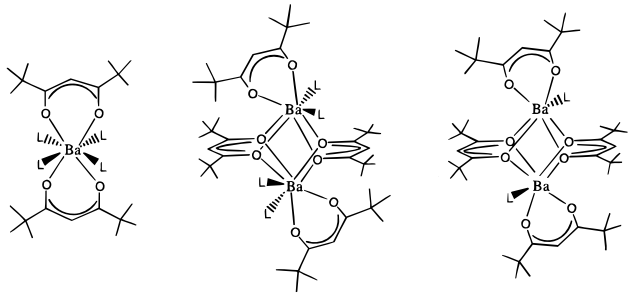

The mononuclear nature of $Ba(thd)_2(THF)_4$ and $Sr(thd)_2(THF)_4$ is most unexpected. The strong tendency of group II complexes to aggregate into multinuclear species, as a means to saturate the coordination sphere of the metal centers, has been well documented in the literature. Polydentate ligands, such as tetraglyme, *N*,*N*,*N*′,*N*′′,*N*′′-pentamethyldiethylenetriamine, and 18-crown-6 crown ethers were found to facilitate the formation of mononuclear species of Ba and Sr.[4,22,24] Important exceptions include $Ba(thd)_2(MeOH)_2(H_2O)_2$[25] and $M(OAr)_2(THF)_3$[26] (M is Ba, Sr, or Ca and Ar is an aryl group containing two *tert*-butyl groups in *ortho* positions). In the latter complex, the steric bulk of the aryloxide ligand undoubtedly prevents bridging and aggregation. The interesting mononuclear complex $Ba(thd)_2(MeOH)_2(H_2O)_2$ seems very closely related to $Ba(thd)_2(THF)_4$. However, the possibility of stabilization through intramolecular hydrogen bonding cannot be ruled in the case of $Ba(thd)_2(MeOH)_2(H_2O)_2$, while such a stabilization is absent for $Ba(thd)_2(THF)_4$. Hydrogen bonding was found in a related dinuclear complex, $[Ba(thd)_2(Me(OCH_2CH_2)_2OH)]_2$, with bridging thd ligands participating in the hydrogen bonding.[27] It is also likely in the case of $[Ba(thd)_2(NH_3)_2]_2$. Thus, the presence of hydrogen bonding can affect Ba−O distances, nuclearity, and structures of complexes and complicate simple molecular comparisons. Furthermore, protic ligands such as CH_3OH and also Hthd are known to facilitate formation of species in which these ligands are associated within higher nuclearity clusters. Examples include a pseudodimer $Ba(thd)_2(MeOH)_3$·MeOH[28] and trimer $[Sr(thd)_2]_3$·Hthd.[19]

(24) Norman, J. A. T.; Pez, G. P. *J. Chem. Soc., Chem. Commun.* **1991**, 971,
(25) Gleizes, A.; San-Lenain, S.; Heughbaert, M. *C. R. Acad. Sci. Paris, Ser. II* **1992**, *315*, 299.
(26) Tesh, K. F.; Hanusa, T. P.; Huffman, J. C.; Huffman, C. J. *Inorg. Chem.* **1992**, *31*, 5572.
(27) Vaartstra, B. A.; Gardiner, R. A.; Gordon, D. C.; Ostrander, R. L.; Rheingold, A. L. *Mater. Res. Soc. Symp. Proc.* **1994**, *335*, 203.
(28) Gleizes, A.; San-Lenain, S.; Medus, D.; Morancho, R. *C. R. Acad. Sci. Paris, Ser. II* **1991**, *312*, 983.

Table 2. Selected Bond Lengths and Bond Angles for $Ba(thd)_2(THF)_4$ and $Sr(thd)_2(THF)_4$

	$Ba(thd)_2(THF)_4$		$Sr(thd)_2(THF)_4$	
	Selected Bond Lengths (Å)			
M−O(thd)	Ba(1)−O(1)	2.657(6)	Sr(1)−O(1)	2.528(3)
	Ba(1)−O(2)	2.643(6)	Sr(1)−O(2)	2.511(3)
M−O(THF)	Ba(1)−O(3)	2.786(7)	Sr(1)−O(3)	2.655(4)
	Ba(1)−O(4)	2.801(6)	Sr(1)−O(4)	2.662(3)
	Selected Angles (deg)			
O(thd)−M−O(thd)	O(2)−Ba(1)−O(1)	65.02(18)	O(2)−Sr(1)−O(1)	68.99(11)
	O(2)−Ba(1)−O(1A)	120.5(2)	O(2)−Sr(1)−O(1A)	117.22(11)
	O(2)−Ba(1)−O(2A)	155.6(3)	O(2)−Sr(1)−O(2A)	153.46(17)
	O(1A)−Ba(1)−O(1)	156.6(3)	O(1A)−Sr(1)−O(1)	155.09(17)
O(THF)−M−O(THF)	O(3)−Ba(1)−O(3A)	67.4(3)	O(3)−Sr(1)−O(3A)	68.89(18)
	O(4)−Ba(1)−O(4A)	68.1(3)	O(4)−Sr(1)−O(4A)	69.22(15)
	O(3)−Ba(1)−O(4)	116.65(19)	O(3)−Sr(1)−O(4)	116.17(11)
	O(3A)−Ba(1)−O(4)	158.5(3)	O(3A)−Sr(1)−O(4)	156.41(12)

Table 3. Comparison of Interatomic Ba−O Distances in $Ba(thd)_2L_x$ Complexes

	Ba−O(adduct ligand) bond dist (Å)	Ba−O(bridging thd) bond dist (Å)
$Ba(thd)_2(THF)_4$	2.786(7)	
	2.801(6)	
$Ba(thd)_2(MeOH)_2(H_2O)_2$[25]	2.720(4) (H_2O)	
	2.777(3) (MeOH)	
$[Ba(thd)_2(Et_2O)]_2$[23]	2.827(6)	2.826(5)
		2.724(5)
		2.803(4)
		2.770(5)
$[Ba(thd)_2(NH_3)_2]_2$[17]	2.888(6)	2.834(4)
	2.923(5)	2.765(3)
		2.874(4)
		2.776(4)

Interestingly, some tridentate ligands with O donor atoms such as diglyme ($Me(OCH_2CH_2)_2OMe$) and the related alcohol ($Me(OCH_2CH_2)_2OH$) did not provide sufficient encapsulation of the metal atoms, and $Ba(thd)_2$ adducts were found to be dinuclear.[27] The latter complex possesses a structure which is very similar to those of the Et_2O, THP, and NH_3 adducts shown above. Therefore, the ability of THF to stabilize a mononuclear structure is surprising, especially given its structural similarity to THP.

Analysis of the Ba−O interatomic distances from the available structural reports reveals that the Ba−O(adduct) distances are very similar to the Ba−O(bridging thd) distances (Table 3). It seems that shorter Ba−O(adduct ligand) distances resulting from stronger coordination of the ligand can result in elongation of thd bridges leading eventually to their breaking and adopting the mononuclear structure by the compound. Steric bulk is also believed to play a role as Ba and Sr complexes of this type are known to adopt a variety of coordination geometries, in which steric factors appear more important than ligands' binding affinities. It is also interesting to note that while it is generally expected that N donor atoms will form stronger bonds with Ba and Sr centers, this system shows that THF is more efficient than NH_3 at lowering the nuclearity of the group II species.

Although the shorter M−O distance (compared to possible M−O(bridging thd)) indicates the greater strength of THF coordination in $M(thd)_2(THF)_4$ implying thermodynamic stability, the THF ligands are kinetically labile and are easily liberated from crystalline solids at room temperature. This suggests that the thd ligands compete with the THF ligands for coordination sites around the metal centers, resulting in the formation of higher nuclearity species. In all cases, thermal analyses indicated liberation of all the Lewis base ligands and formation of $[M(thd)_2]_x$, as evidenced by the melting endotherms for the respective species.

It is of further interest to consider the utility of $Ba(thd)_2(THF)_4$ and $Sr(thd)_2(THF)_4$ as CVD precursors for the deposition of oxide thin films. These complexes display very low melting points, and therefore, are attractive for liquid delivery CVD. On the other hand, the poor thermal stabilities of these THF adducts suggest that these species are likely to undergo ligand dissociation during delivery to the CVD reactor. It seems necessary, therefore, to provide excess THF, i.e., employ liquid delivery CVD with THF as the solvent. The presence of excess THF vapors is likely to result in shifting equilibria toward the mononuclear species. Polyethers and polyamines can serve the same purpose, but in typical applications they are provided as additives in relatively small excess and not as the solvent. Using THF as both the solvent and Lewis base ligand can be beneficial to the transport and vaporization by suppressing precursor aggregation leading to increased nuclearity. The presence of mononuclear species is strongly preferred for CVD applications, even when the Lewis base ligands can be readily liberated during heating.

Supporting Information Available: X-ray crystallographic files in CIF format for the structure determinations of $Sr(thd)_2(THF)_4$ (**1**) and $Ba(thd)_2(THF)_4$ (**2**). This material is available free of charge via the Internet at http://pubs.acs.org.

IC990641Z